

# Peroxy radical observations over West Africa during AMMA 2006: photochemical activity in the outflow of convective systems

M. D. Andrés-Hernández<sup>1</sup>, D. Kartal<sup>1</sup>, L. Reichert<sup>1</sup>, J. P. Burrows<sup>1</sup>, J. Meyer Arnek<sup>2</sup>, M. Lichtenstern<sup>3</sup>, P. Stock<sup>3</sup>, and H. Schlager<sup>3</sup>

<sup>1</sup>Institute of Environmental Physics, University of Bremen, Germany

<sup>2</sup>German Remote Sensing Data Center (DFD), Oberpfaffenhofen, Germany

<sup>3</sup>Institute of Atmospheric Physics, German Aerospace Center (DLR), Oberpfaffenhofen, Germany

Received: 17 November 2008 – Published in Atmos. Chem. Phys. Discuss.: 16 January 2009

Revised: 28 April 2009 – Accepted: 19 May 2009 – Published: 5 June 2009

**Abstract.** Peroxy radical measurements made on board the DLR-Falcon research aircraft over West Africa within the African Monsoon Multidisciplinary Analysis (AMMA) campaign during the 2006 wet monsoon are presented in this study. The analysis of data focuses on the photochemical activity of air masses sampled during episodes of intense convection and biomass burning. Generally, the total sum of peroxy radical mixing ratios, measured in the outflow of convective clouds, are quite variable but occasionally are coupled with the NO variations indicating the coexistence or simultaneous emission of NO<sub>x</sub>, with a potential radical precursor (i.e. formaldehyde, acetone or peroxides), which has likely been transported to higher atmospheric altitudes. Based on the measurements, significant O<sub>3</sub> production rates around 1 ppb/h in the MCS outflow are estimated by using a box model with simplified chemistry. Peroxy radicals having mixing ratios around 20–25 pptv and with peak values of up to 60–70 pptv are measured within biomass burning plumes, detected at the coast in Ghana. Calculations of back-trajectory densities confirm the origin of these air masses being a biomass burning region at southern latitudes and close to the Gulf of Guinea, according to satellite pictures.

Measured peroxy radical concentrations agree reasonably with modelled estimations taking into account simple local chemistry. Moreover, the vertical profiles taken at the aircraft base in Ouagadougou, Burkina Faso, indicate the common feature of having maximum concentrations between 2 and 4 km, in agreement with other literature values obtained under similar conditions.

## 1 Introduction

Hydroperoxyl (HO<sub>2</sub>) and alkyl peroxy (RO<sub>2</sub>; R=organic chain) radicals, are involved in most of the oxidation mechanisms taking place in the troposphere. Knowledge of their amounts and distributions provides essential information about the aging and history of an air mass. In spite of their importance in the chemical processing of the troposphere, only a very limited number of measurements are available in the literature. This arises from their high reactivity, which complicates their measurement and results in small mixing ratios. Measurements of tropospheric free radicals are particularly scarce between 30 degrees South and 30 degrees North as reported by Cantrell et al. (2003a).

The mesoscale convective systems (MCS) enclosed into synoptic-scale African Easterly Waves during the West African Monsoon are considered to be the origin of about 40% of the Atlantic tropical cyclones and responsible for troposphere-stratosphere exchange (Agustí-Panareda, and Beljaars, 2008). Africa is therefore a suitable environment for investigating the photochemical activity in air masses impacted by MCS. Little is known about the chemical composition of these air masses during intense convective episodes. The outflow boundary of a MCS is a suitable environment for lifting, leading to effective transport of trace gases, aerosols and water vapor from the boundary layer into the free atmosphere. It is expected that the vertical transfer of oxygenated hydrocarbons and peroxides lead to enhanced O<sub>3</sub> formation as the peroxy radicals produced by UV photolysis react rapidly with NO which has also been vertically and horizontally transported, or produced by lightning. The total yield depends on UV radiation, potential losses of radicals (aerosols, clouds) and the vertical budget of radical precursors (Lelieveld and Crutzen, 1994; Cantrell et al., 2003a, c).



Correspondence to: M. D. Andrés Hernández  
(lola@iup.physik.uni-bremen.de)

In particular acetone can both be a source of peroxy and alkoxyradicals and affect the partitioning of odd nitrogen between NO, NO<sub>2</sub> and PAN (McKeen et al., 1997).

HO<sub>x</sub> in the upper troposphere (6 to 12 km) cannot generally be sustained by the primary production of OH from the reaction of O<sup>1</sup>D, produced by the photolysis of O<sub>3</sub> with H<sub>2</sub>O and the subsequent reactions of OH with CO and O<sub>3</sub>. Transported HO<sub>x</sub> precursors other than O<sub>3</sub> and H<sub>2</sub>O seem to be the primary sources of hydrogen containing radicals in much of the upper troposphere (Wennberg et al., 1998). In the presence of enough NO from lightning, biomass burning, and aircraft emissions the resultant catalytic mechanism can be responsible for rapid and effective production of O<sub>3</sub> in the higher layers of the atmosphere and have a global impact (Jaeglé et al., 2001). Prather and Jacob (1997) suggested that given a 10 days overturning rate of the tropical upper troposphere, deep convection could cause a persistent chemical imbalance in HO<sub>y</sub> (defined as OH, HO<sub>2</sub> and their non-radical reservoirs, i.e., HO<sub>y</sub>=OH+peroxy+2H<sub>2</sub>O<sub>2</sub>+2CH<sub>3</sub>OOH+HNO<sub>2</sub>+HNO<sub>4</sub>). This has also been confirmed by the measurements of peroxides and CH<sub>3</sub>OOH of Cohan et al. (1999) in aged convective outflows in the tropical Pacific. Conversely, HO<sub>x</sub> greater than the model predictions for high NO regimes (500–600 pptv) have been measured in biomass burning plumes encountered over the western Pacific equatorial region (Folkins et al., 1997) Similarly, unexpected high OH concentrations have been measured over the pristine Amazon forest (Lelieveld et al., 2008). It has been proposed that natural isoprene oxidation recycles OH efficiently in low NO<sub>x</sub> air through reactions of organic peroxy radicals.

The Institute of Environmental Physics of the University of Bremen (IUP-UB) participated in the AMMA measurement campaign taking place during the wet monsoon season in August 2006. IUP-UB contributed with the measurement of the total sum of peroxy radicals (RO<sub>2</sub>\*=HO<sub>2</sub>+RO<sub>2</sub>) onboard of the German DLR-Falcon. This was part of a suite of measurements from aircraft, ground stations and satellites to study the composition and the oxidative capacity of air masses over West Africa with special focus on the impact of MCS within the monsoon period (Reeves et al., 2009). In addition, biomass burning plumes were observed during the measurement campaign.

Six DLR-Falcon flights were conducted from Ouagadougou in Burkina Faso (12.15° N 1.30° W) in the period from 1 to 18 August 2006. An overview of the aircraft campaign and details of the flights are described in Reeves et al., 2009.

## 2 Experimental

RO<sub>2</sub>\* was measured by using an airborne PERCA (PEroxy Radical Chemical Amplifier) instrument, with a double detector, i.e., a dual channel airborne peroxy radical chemi-

cal amplifier (DUALER). PERCA is one of the most frequently used measurement technique for the total sum of peroxy radicals. The method has been gradually characterised and improved and there is abundant literature about its deployment for ground based measurements in diverse polluted and remote areas (e.g. Cantrell et al., 1996a; Monks et al., 1996; Carslaw et al., 1999; Burkert et al., 2001a–b, 2003; Hernández et al., 2001; Volz-Thomas et al., 2003; Zanis et al., 2003; Fleming et al., 2006a–b). In most of the cases, the measurement system consists of a single reactor and detector. However, for remote areas and airborne measurements, dual systems comprising two identical reactors and one or two detectors have been developed in order to increase sensitivity and accuracy in the case of rapid changing background concentrations which can interfere in the radical determination (Cantrell et al., 1996b; Green et al., 2003). Briefly, the DUALER utilises the simultaneous detection of the NO<sub>2</sub> mixing ratios by two identical reactors using a common sampling line. NO and CO are alternatively added to the reactors in such a way that the chemical conversion of RO<sub>2</sub>\* into NO<sub>2</sub> in a chain reaction takes place in one reactor (amplification mode) while the other measures the NO<sub>2</sub> background, i.e., the NO<sub>2</sub> present in the air sampled plus the NO<sub>2</sub> originating from all other sources up to the detector such as reaction of NO with O<sub>3</sub>, the decomposition of PAN, etc. (background mode). The modes of the reactors are switched every 60 s. NO<sub>2</sub> is measured by detecting the light emitted from the chemiluminiscent reaction of NO<sub>2</sub> with a solution of Luminol. Provided that the length of the chain reaction for the reactors (CL: chain length) is known, the difference in the signal of the detectors (amplification-background) can be related quantitatively to the RO<sub>2</sub>\* content in the air sampled. More details about the instrument principle, characteristics, performance and characterisation are provided elsewhere (Kartal et al., 2009).

### 2.1 Critical aspects of the measurement of peroxy radicals

In previous studies it has been shown that the CL of the PERCA decreases with the pressure (Kartal et al., 2009). For this reason the DUALER is maintained at a constant pressure, lower than the ambient, during the measurement in the aircraft, and the corresponding CL is determined in the laboratory. In order to cover the range of the pressure levels during the flights but still keeping a reasonable detection limit, 200 mbar was the pressure selected for the AMMA campaign. A pressure gradient  $\Delta P = P_{\text{ambient}} - P_{\text{DUALER}}$  of 70 mbar is required for successful measurement. This limits somewhat the amount of RO<sub>2</sub>\* data available during the flights for the characterisation of the MCS outflow which were often carried out at altitudes corresponding to pressure levels lower than 250 mbar.

Concerning the vertical profiles of trace gases taken by the DLR-Falcon, it is important to note that the aircraft normally

remains at each single pressure level only for a few minutes. This normally leads to poor statistics of the  $RO_2^*$  measurement signals, especially in the case of unexpected variations in the concentrations.

Another critical aspect of the DUALER measurements during AMMA is related to the  $NO_2$  calibrations of the detectors. The concentration of the  $NO_2$  gas cylinder built in the DUALER for calibrations was not stable during the campaign. This is attributed to the high temperatures and humidity reached in the aircraft prior to the flight which possibly led to changes in the wall losses in the pressure regulator and gas tubing in spite of lengthy flushing of the gas lines. This resulted in inconsistent in-flight  $NO_2$  calibration of the detectors, which could only be calibrated before and after the measurement flight.

To overcome these issues and to monitor potential changes in the sensitivity of the detector during the flight, a mathematical method based on the  $O_3$  concentrations simultaneously measured on the DLR-Falcon has been developed. Provided that the  $NO_2$  background is essentially defined by the ambient  $O_3$  mixing ratios and that the response of the luminal detector remains linear (i.e.,  $NO_2 = aX + b$ ), the sensitivity of each detector for each single point  $k$  during a selected time interval can be calculated from two consecutive  $O_3$  measurements at the time  $k$  and  $k+1$ . In order to rule out errors related to a malfunction of the  $O_3$  instrument or to sudden variations of background ambient gases other than  $O_3$  but providing  $NO_2$  to the DUALER, a careful analysis of the involved parameters is made, and the error for any particular selected time interval is determined. The mathematical procedure and propagation of errors is described more in detail in Kartal et al. (2009).

The total error associated to the measurement of  $RO_2^*$  is defined by the uncertainties in the determination of the  $NO_2$  detector sensitivity and of the chain length. Laboratory  $NO_2$  calibrations with cylinders of known concentration have generally a reproducibility within 99%. By using the procedure described in Kartal et al. (2009), based on  $O_3$  measurements, the relative accuracy of the  $NO_2$  airborne measurements remains between 20% and 35%. Concerning the CL, its laboratory determination at a particular pressure is subject to a 15% standard deviation.

The propagation of the errors above leads to a total error between 25 and 45% for the  $RO_2^*$  measurements performed during AMMA, depending on the flight conditions and the stability of the measurement signals for any particular measurement interval. Potential in-flight losses of radicals in the reactor before reaching the addition points caused by the presence of clouds or aerosols can only be estimated.

## 2.2 Data from other instrumentation

The analyses of the air masses undertaken in this study used measurements of other constituents and parameters made aboard the DLR-Falcon. These data are provided by the

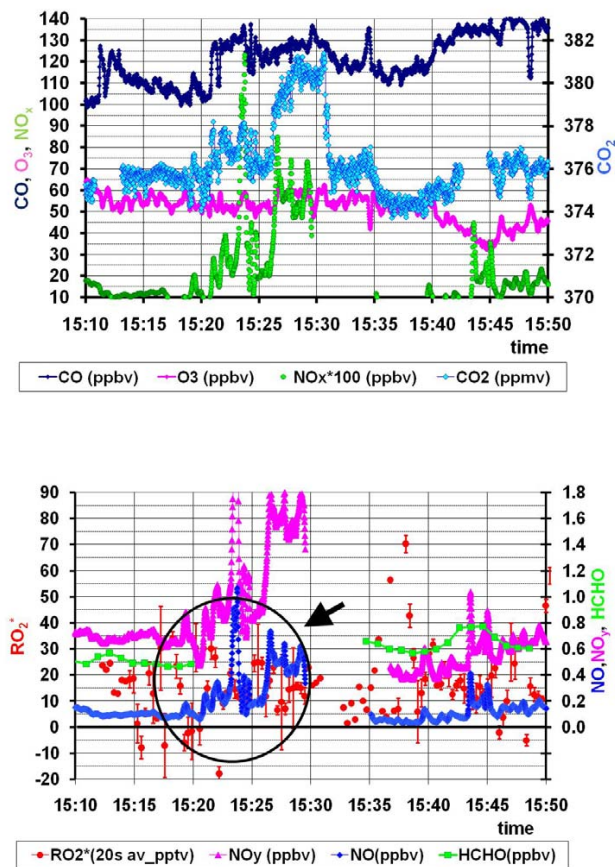


**Fig. 1.** Trace gas measurements during crossing of a pollution plume during the DLR-Falcon flight carried out on the 15 August 2006. The measurements were taken at the 260 mbar pressure level. An episode of coincident  $RO_2^*$  and NO variations is highlighted.

DLR-Institute of Atmospheric Physics.  $O_3$  and  $CO_2$  were measured using UV and IR absorption techniques, respectively (Schlager et al., 1997; Schulte et al., 1997). CO was detected with an UV fluorescence instrument (Gerbig et al., 1996). Reactive nitrogen compounds (NO,  $NO_y$ ) were measured using two  $O_3/NO$ -chemiluminescence detectors and a gold converter for reduction of higher oxidized  $NO_y$  compounds to NO (Schlager et al., 1997; Ziereis et al., 2000). Formaldehyde, HCHO, was detected by a fluorometric technique (Hantzsch reaction). Characteristics of the instruments (accuracies, detection limits) are summarized in Reeves et al., 2009.

## 2.3 Supporting calculations

Clusters of back trajectories have been launched in the vicinity of the aircraft location to gain additional information about the origin of the air masses sampled within the case studies. The trajectory calculations were made using the

FLEXTRA model (Stohl et al., 1995, 1998). In order to account for uncertainties in the meteorological data, these trajectory clusters were released from a volume of  $0.6 \times 0.6$  degrees (horizontally)  $\times 1000$  m (vertically)  $\times 1$  h (time) centred at the aircraft position and time of the corresponding measurements. All back trajectories are followed for 72 h. The trajectory density, i.e., the number of trajectories passing a certain volume of air, has been additionally determined. For the analysis of AMMA data the trajectory density bases on a grid of  $0.25^\circ \times 0.25^\circ \times 100$  m. Subsequently the trajectory densities are normalised to 1 to derive a quantity which is independent from the actual number of trajectories discussed for the specific case study. This step is performed for each 2-dimensional projection independently. A similar approach is reported by Eneroth et al. (2003). Furthermore, the Lagrangian Boxmodel BRAPHO (BRemen Atmospheric PHOtochemical model) (Meyer-Arnek, 2005) has been used to analyse the photochemical evolution of the probed trace gases. BRAPHO calculates the chemistry within a closed volume of air, on the basis of the Master Chemical Mechanism (MCM) (Saunders et al., 2003). For the present work, a simplified photochemistry (see Appendix A) was used for the estimation of the local  $O_3$  production under the measurement conditions. The simulations are initialised with the corresponding measurements taken on board the DLR- Falcon.

### 3 Results

Air masses of different photochemical activity were sampled during the AMMA measurement campaign. In addition to measurement uncertainty, there are many physical and chemical factors which control the variations of the  $RO_2^*$  observed, e.g. the different composition of air masses transported from different source regions, the variations in the actinic radiation fields, possible loss reactions in the presence of clouds etc. Within the same pressure level, chemical episodes with different balance between controlling variables can often be distinguished. Generally, change of pollution plume type is indicated by short term variations of  $NO_x$ ,  $NO_y$ ,  $CO_2$  and  $CO$  concentrations. As a surrogate for the volatile organic compounds (VOC), HCHO was measured by the instrument payload on the DLR-Falcon. The HCHO data coupled with the variations of  $CO$  and  $CO_2$  can be used to identify the arrival of air masses of different origins and likely different loading of VOCs.

In Fig. 1 the trace gases measured at the 260 mbar pressure level during the DLR-Falcon flight on the 15 August 2006 are shown demonstrating the chemical complexity of air masses observed during AMMA. The objective of the flight was to probe the outflow of a MCS over northern Benin. The DLR-Falcon remained at the same pressure level between 15:02 and 15:52 h. While  $j_{NO_2}$  does not indicate significant variations in the cloud cover, the trace gas concentrations change considerably. Between 15:20 and 15:30 h  $CO$  sharply in-

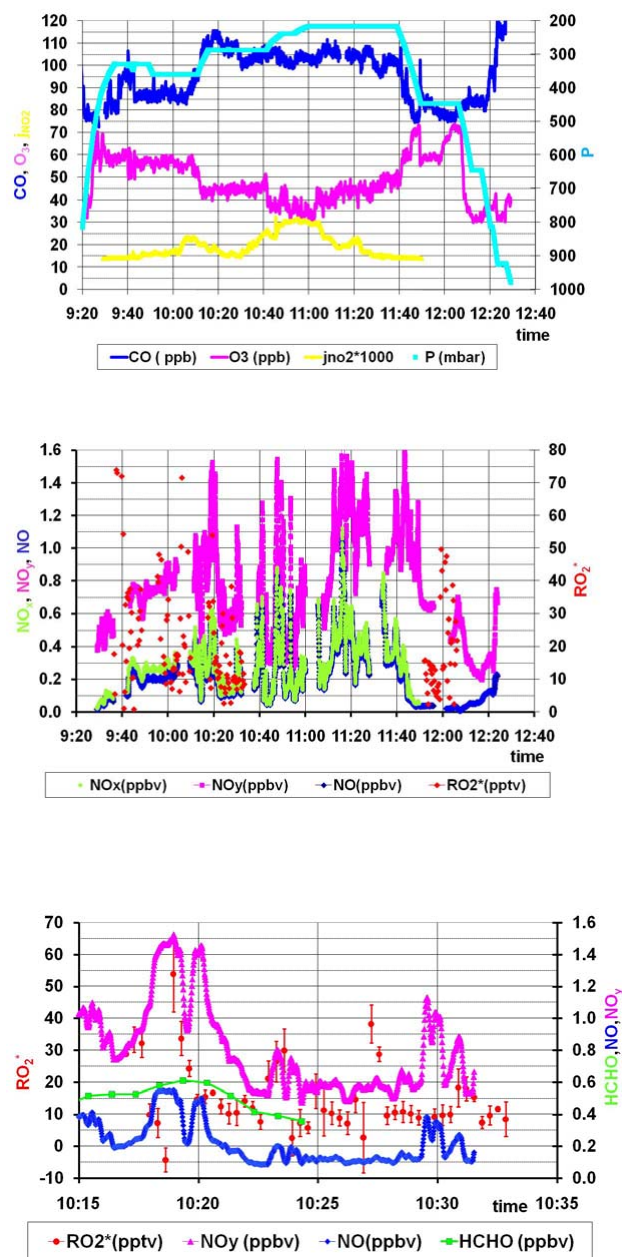


**Fig. 2.** Trace gas mixing ratios measured during the DLR-Falcon flight on the 15 August 2006. The bottom plot shows in detail the  $RO_2^*$  mixing ratios measured at 287 mbar. The depicted error bars only represent the statistical error of the 20 s  $RO_2^*$  averages.

creases up to 135 ppbv while  $NO$  and  $NO_y$  rise above the background level and show high variability up to 1.2 and 2.2 ppbv respectively.  $RO_2^*$  generally show high variability and are anticorrelated to  $NO$  variations as expected according to the known chemistry, i.e., the formation of  $RO_2^*$  via reaction of  $CO$  (and/or  $VOC$ ) with  $OH$  in the presence of  $H_2O$ , and the depletion in the presence of  $NO_x$  by loss

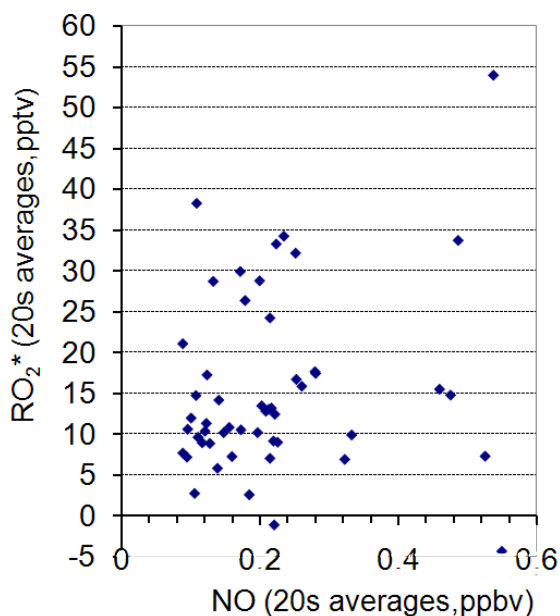


**Fig. 3.** RO<sub>2</sub>\* and NO observed on the 15 August 2006 at the 287 mbar level.

reactions (see CO and CH<sub>4</sub> oxidation in Appendix A). However, RO<sub>2</sub>\* occasionally follow quite closely (see Fig. 1) the NO behaviour. These simultaneous increases in CO, CO<sub>2</sub>, NO/NO<sub>y</sub>, RO<sub>2</sub>\* and O<sub>3</sub> are indicative of local photochemical activity being triggered by fresh emissions of potential radical precursors together with the emission and/or transport of NO<sub>x</sub> and other pollutants. The in situ production of radicals and subsequent reaction with the present NO leads to O<sub>3</sub> production. Box model calculations initialised with the conditions observed at 15:25 h indicate that the radical chemistry in the air mass is responsible for an O<sub>3</sub> production of approximately 1.0 ppb h<sup>-1</sup>. This value is in reasonable agreement with the 4–8 ppb day<sup>-1</sup> production rates calculated by other modeling studies in MCS outflows during AMMA assuming different VOC and dilution patterns (Schlager et al., 2009). Cooper et al. (2006) reported large upper tropospheric O<sub>3</sub> enhancements up to 24 ppbv above midlatitude North America during the summer, and estimated an 80% contribution from in situ O<sub>3</sub> production from lightning and a 20% contribution from O<sub>3</sub> transport from the surface or in situ production from other sources of NO<sub>x</sub>. Lower O<sub>3</sub> production rates have been observed in the upper troposphere in other seasons. Jaeglé et al. (1999) calculated O<sub>3</sub> production rates up to 2 ppb day<sup>-1</sup> for the measurements taken at 8–12 km during the SONEX campaign over the North Atlantic in winter. Miyazaki et al. (2003) estimated 0.5–4.4 ppbv day<sup>-1</sup> net O<sub>3</sub> production rates in the upper troposphere over East Asia in springtime.

The focus of this manuscript is the analysis of RO<sub>2</sub>\* for selected episodes and behaviours observed during AMMA.

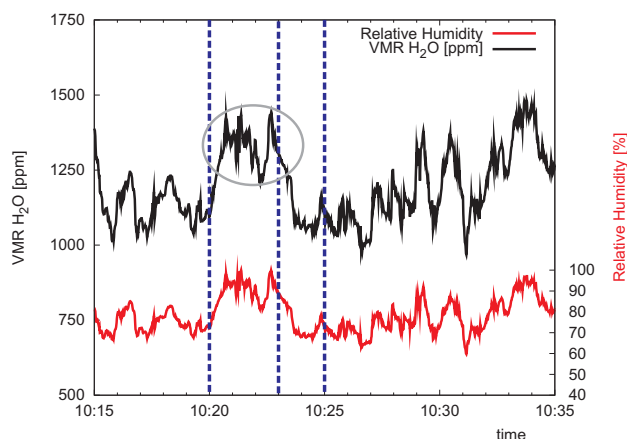


**Fig. 4.** Water vapor observed on the 15 August 2006 at the 287 mbar level. The higher humidity values between 10:20 and 10:24 confirm the presence of air masses affected by convection. The time points selected for the box model initialisation are also highlighted.

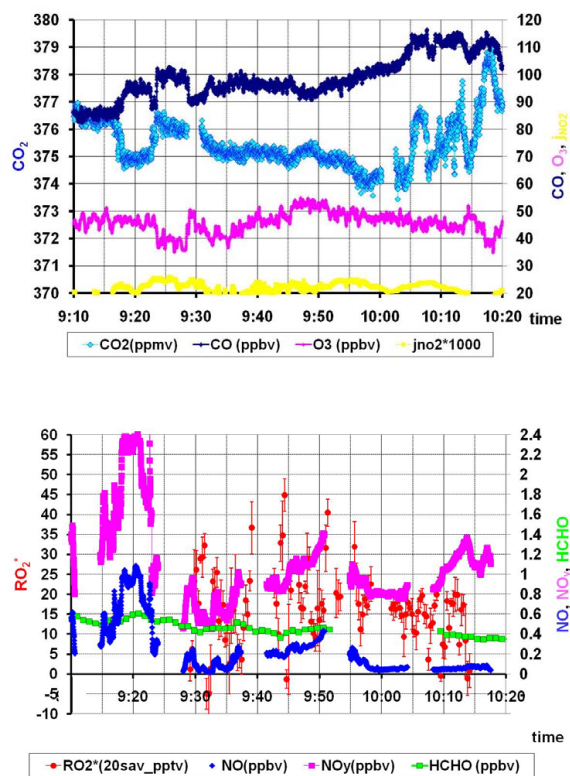
Specifically convective outflow from clouds, biomass burning plumes and the vertical distributions observed above Ouagadougou were selected for study.

### 3.1 RO<sub>2</sub>\* measurements within convective episodes

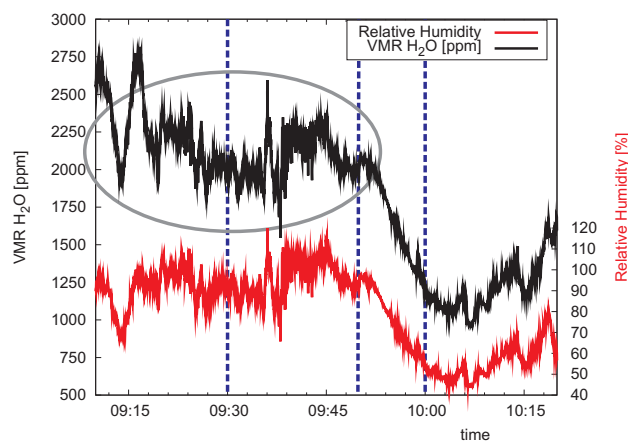
Data obtained during the first flight on the 15 August 2006 are depicted in Fig. 2. The objective of the flight was to measure the outflow of a MCS located over Mali after passing Ouagadougou the evening before. The DLR-Falcon reached this outflow area at the 287 mbar pressure level. The NO<sub>y</sub> and NO<sub>x</sub> data measured during the flight (Fig. 2b) show the typical signature of high variable concentrations within this kind of convective outflow. CO remains at 100–110 ppbv, about 20 ppbv higher than outside the outflow area. As mentioned in Sect. 2.1, RO<sub>2</sub>\* measurements are only available for pressures >250 mbar.

Figure 2c focuses on the RO<sub>2</sub>\* results, which on the average remain about 10 pptv. The increase of RO<sub>2</sub>\* with NO up to the 0.5 ppbv maximum (Fig. 3), and the similarity of the RO<sub>2</sub>\* and NO variation patterns are remarkable. Rather it is expected that RO<sub>2</sub>\* decrease as NO increases because the sink reactions of radicals with NO<sub>x</sub> are gaining in importance. The observed behaviour thus indicates the presence of a radical precursor being emitted simultaneously with NO. This could be a peroxy radical source, either transported by convection from another region and/or locally produced. O<sub>3</sub> remains practically constant at 45 ppbv for the whole period.

The convective injection of peroxides has been suggested to be a source of HO<sub>2</sub> radicals (Prather et al., 1997; Cohan et al., 1999; Jaeglé et al., 1997a; Faloon et al., 2000). The convective pumping of carbonyl compounds like formaldehyde, acetaldehyde or acetone may also be responsible for local production of RO<sub>2</sub>\*. Faloon et al. (2000), already



**Fig. 5.** Trace gas mixing ratios measured during the DLR-Falcon flight on the 4. August 2006. The outflow of the MSC is reached at the 315 mbar pressure level (09:17 h). The depicted  $RO_2^*$  error bars represent only the statistical error of the 20 s averages.



**Fig. 6.** Water vapor measured during the DLR Falcon flight on the 4 August 2006. The convection zone is left at 09:50 h. Times selected for the box model initialisation are highlighted.

reported on unexpected  $HO_2$  values in different masses in the upper troposphere (at or above 6 km) in the presence of  $100 < NO < 500$  pptv. These authors interpret the model underestimation of the  $HO_2$  as a possible unmeasured  $HO_x$

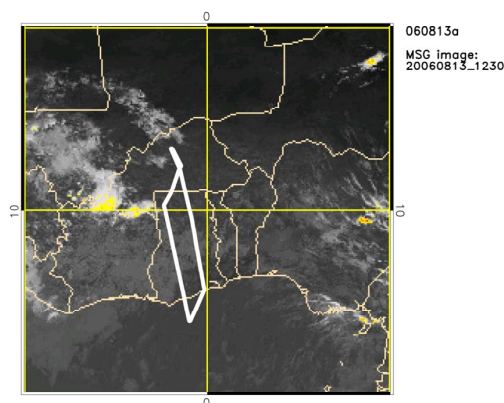
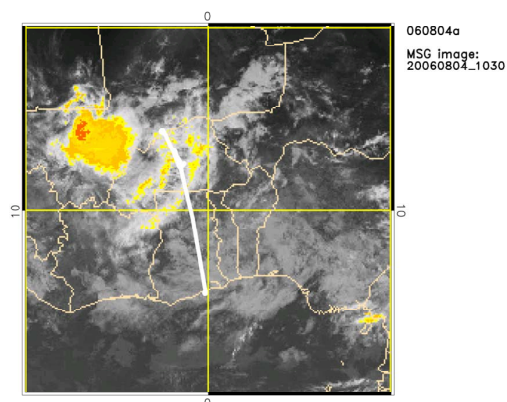


**Fig. 7.** DLR-Falcon flight tracks on the 4 August 2006 and the 13 August 2006.

source that happened to be spatially correlated with  $NO_x$ , independent of its origin. A similar underestimation has also been reported both for  $HO_2$  and  $HO_2 + RO_2$  measurements performed during the TRACE-P campaign by using Peroxy radical Chemical Ionization Mass Spectroscopy (PerCIMS) (Cantrell et al., 2003b). Similarly, acetone seems to explain most of the missing  $HO_x$  in models for  $H_2O < 25$  to 30 ppm in the upper troposphere over the Pacific (McKeen et al., 1997).

$HCHO$  was measured on the DLR-Falcon at this pressure level only up to 10:24 h (Fig. 2c). The general  $HCHO$  behaviour agrees roughly with the  $NO$ ,  $NO_y$  and  $RO_2^*$  patterns but it is not possible to definitely assign some of the short term  $RO_2^*$  variations to this potential  $HO_2$  precursor, as  $HCHO$  is measured with lower time resolution. On the other hand  $H_2O$  remained around 1000 ppm at the 287 mbar pressure level. However, as the  $NO$  to  $NO_2$  ratio is relatively high (between 7 and 9) if acetone would be present, it should be quite effective in the production of  $HO_x$ , as the competing reaction of the formation of peroxyacetyl nitrate (PAN) is favoured by low  $NO$  to  $NO_2$  ratios.

Temporal variations in humidity confirm local inhomogeneity caused by the convection at this pressure level.

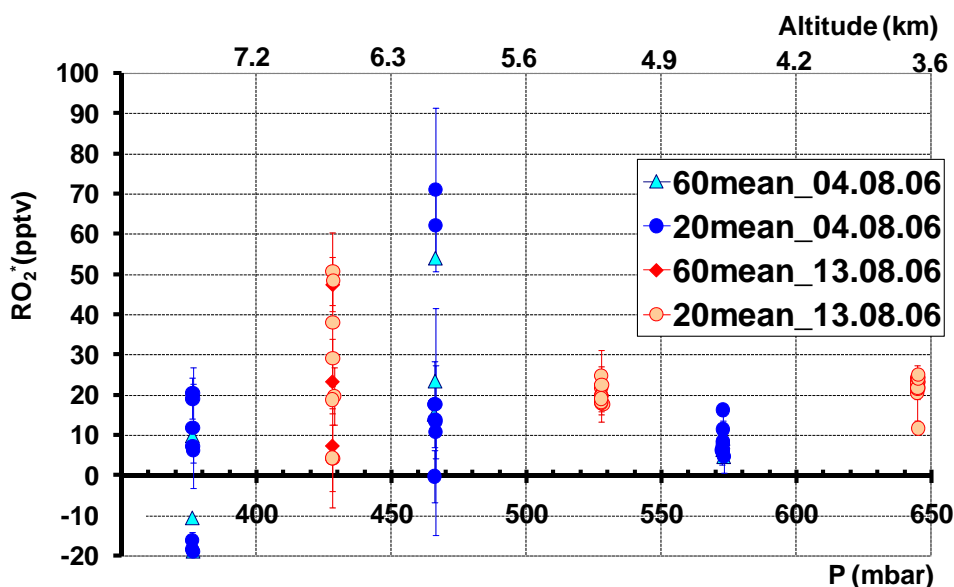
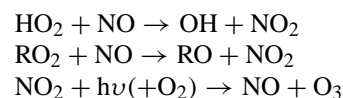


**Fig. 8.** Peroxy radical mixing ratios measured on the 4 August 2006 and 13 August 2006 coastal vertical profiles. The statistical error of the corresponding 60 s and 20 s averages is depicted.

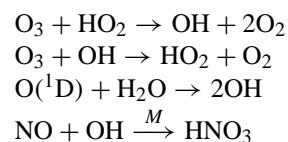
Increases in humidity at the 10 km flight altitude indicate air masses being uplifted by convection (Fig. 4). This has an effect in the local chemistry which might be responsible for the variability of the  $\text{NO}_x$  and  $\text{RO}_2^*$  in situ values.

Bechara et al. (2009) recently presented vertical isoprene profiles measured during the AMMA campaign on board the French Falcon. Their results provide evidence for the impact of the deep convection on the composition of short lived VOC in the upper troposphere. Isoprene mixing ratios up to 0.3 ppbv were detected between 8–11 km altitudes, in spite of its biogenic origin and less than 2 h life time. In order to estimate the impact of isoprene as an in situ source of peroxy radicals, the reaction mechanism for isoprene decomposition suggested by Meyer-Arnek et al. (2005) was included in the box model presented in Appendix A. It is based on the simplification of the chemistry in the Master Chemical Mechanism version 3.1 (Saunders et al., 2003) focusing on the species being either involved in the  $\text{NO}_x$ - $\text{HO}_x$ -cycle or in the isoprene decay.

Once the radicals are produced, the net  $\text{O}_3$  production comes from the competition between formation:



and  $\text{O}_3$  loss reactions:



Different model runs were performed for different  $\text{NO}_x$  and isoprene mixing ratios representative of the observations. According to these, the injection of 0.1 to 0.2 ppbv isoprene in to the upper tropospheric layers can be directly responsible for an increase up to 6–7 times in the amount of peroxy radicals. In the presence of  $\text{NO}_x$  mixing ratios varying between 0.2 and 0.6 ppb the so formed peroxy radicals lead to a 20–25% increase in the net  $\text{O}_3$  production. These results are in reasonable agreement with the measurements.

In order to obtain a representative picture of the photoactivity of the air mass within the MCS outflow and at this pressure level as a whole, the  $\text{O}_3$  production rate was estimated for three different cases by initialising the box model with the measurements at 10:20, 10:23 and 10:25 h. These simulations lead to  $\text{O}_3$  production rates of 3.5, 1.1 and 0.2 ppb  $\text{h}^{-1}$ , respectively. These values agree reasonably with the simulations in MCS outflow reported by Schlager et al. (2009).

Another example of convective outflow is given by the flight on the 4 August 2006. At the 315 mbar pressure level the DLR-Falcon sampled the outflow of the MCS which has passed over Niamey the day before (Fig. 5). The aircraft remained within the MCS outflow until approximately 09:50 h while keeping the pressure level until circa 10:20 h. This is clearly confirmed by the variation of the absolute humidity with a clear decrease in the values when leaving the outflow zone (Fig. 6).  $\text{NO}$  and  $\text{NO}_y$  are highly variable reaching 2.5 and 1.2 ppbv, respectively, at the beginning of the level around 9:15 h. At this point  $\text{RO}_2^*$  remain undetectable until  $\text{NO}$  decreases to the 0.2–0.5 ppbv level around 09:30. The increase in the  $\text{NO}/\text{NO}_y$  ratio from 0.04 to 0.5 indicates the presence of relatively fresh emissions. Similarly to the

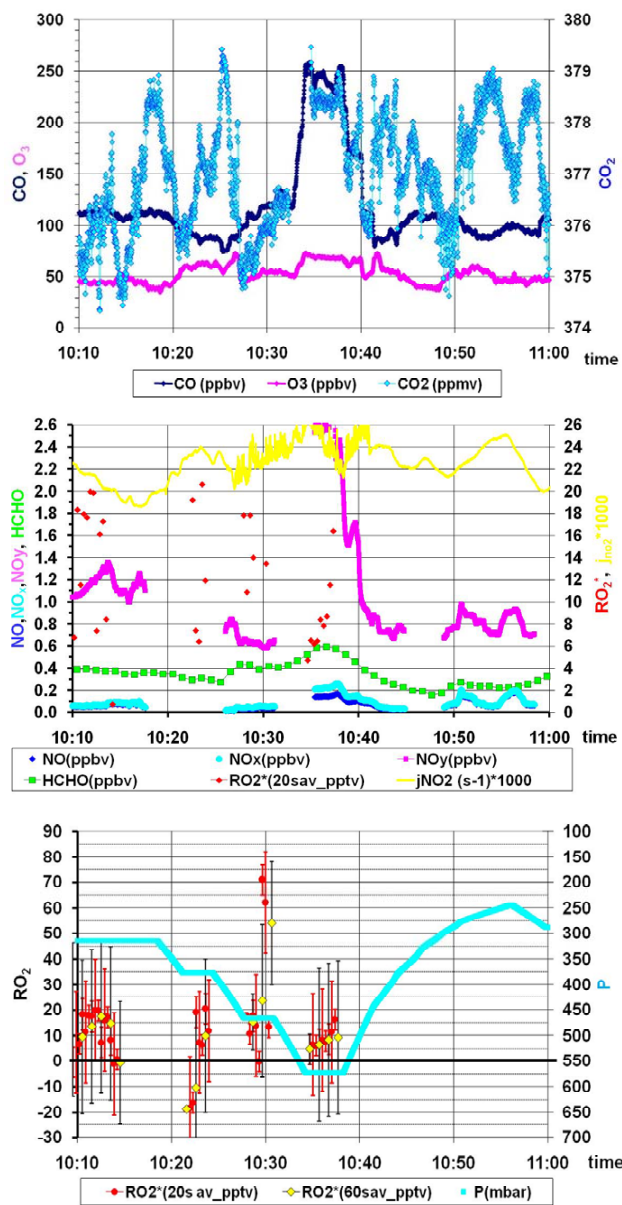


**Fig. 9.** Trace gas mixing ratios measured during the coastal vertical profile on the 4 August 2006. The statistical error of the 20 s and 60 s  $RO_2^*$  averages is also depicted.

15 August 2005, the potential transport of acetone simultaneous to NO would favour the production of radicals, as the NO/NO<sub>2</sub> ratio remains relatively high (around 7) most of the time. This might explain the variability of the  $RO_2^*$  mixing ratios, occasionally following the NO variations and reaching up to 40 pptv. The error bars depicted in Fig. 5b correspond to the standard deviation of the 20 s averages from the 1 s original data. The total error of the  $RO_2^*$  20 s averages is estimated to be within 45%. As mentioned in the Sect. 2.1 and described more in detail elsewhere (Kartal et al., 2009), the

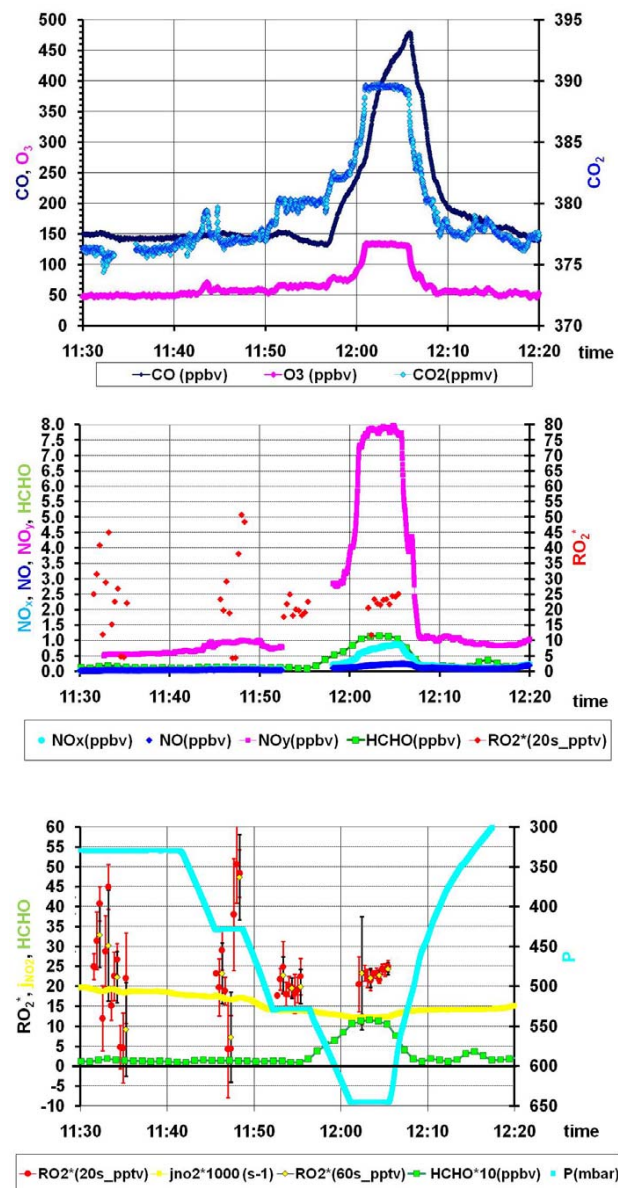


**Fig. 10.** Trace gas mixing ratios measured during the coastal vertical profile on the 13 August 2006. The statistical error of the 20 s and 60 s  $RO_2^*$  averages is also depicted.

total  $RO_2^*$  error partly depends on the quality and variability of the O<sub>3</sub> measurements and therefore varies for any particular measurement interval. The presence of clouds likely introduces some additional data variability. The role of clouds as sink of radicals has been often discussed in the literature but still requires further clarification (Seigneur and Saxena, 1985; Mauersberger, 1995; Buxton and Salmon, 2003; Shi et al., 2003).

No obvious correlation with HCHO is observed. However, as the DUALER measures the total sum of peroxyradicals,

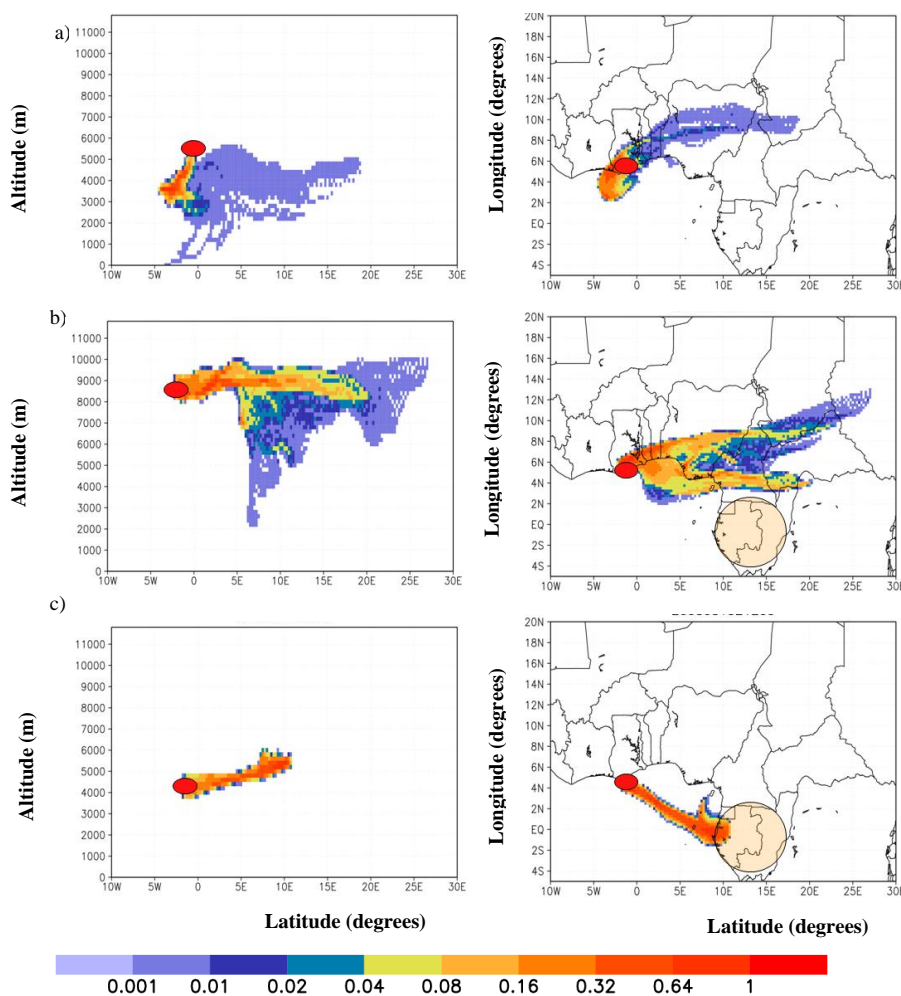


**Fig. 11.** Trajectory densities calculated for the vertical profile measured on the (a) 4 August 2006 at 10:30 h (b) 13 August 2006 at 11:40 h and (c) 13 August 2006 at 12:05 h. The BB area according to satellite data is highlighted.

the absence of a strong correlation does not directly rule out that a fraction of  $\text{HO}_x$  is formed from HCHO. Nor can the presence of other sources of radicals from the oxidation of organic compounds be excluded, as above discussed for isoprene. Vertical transport from the layers below seems to be the most likely explanation of the observed NO. As presented in the summary of the AMMA observations by Reeves et al. (2009), the general pattern in the trace gas concentrations observed along the whole latitude range measured is indicative of the transport by convection to higher altitudes. The pattern comprises two layers of higher mixing ratios, one close to the surface up to 900 hPa and another at higher altitudes. Similar results are recently reported by Ancellet et al. (2008). For NO, given the low mixing ratios measured within the boundary layer close to the surface (Reeves et al., 2009), this transport must be enhanced by  $\text{NO}_x$  from lightning, which is expected during storm episodes within deep convective clouds.

After leaving the convective zone around 10:00 h, CO in-

creases gradually from 90 to 120 ppbv,  $\text{CO}_2$  from 374 up to 379 ppmv, NO decreases to zero and the  $\text{RO}_2^*$  variability diminishes notably ( $\text{RO}_2^*$ : 5–25 pptv).

The box model was initialised with the measurements at 09:30, 09:50 and 10:00 h representing different  $\text{RO}_2^*/\text{NO}$  ratios within and outside the MCS convective outflow. These simulations lead to a local  $\text{O}_3$  production rate between 0.4 and  $1.2 \text{ ppb h}^{-1}$  in the MCS outflow and  $0.17 \text{ ppb h}^{-1}$  outside the convection outflow. These local production rates are likewise within the values reported by Schlager et al. (2009).

### 3.2 Biomass burning plumes

Figure 7 shows the flight tracks on the 4 and 13 August 2006. On both days a vertical profile was taken as the DLR- Falcon reached the coast in Ghana.

The measured  $\text{RO}_2^*$  vertical profiles, based on 20 s and 60 s data averages are shown in Fig. 8. The concentration of other trace gases, especially CO and  $\text{CO}_2$  (Figs. 9 and 10)

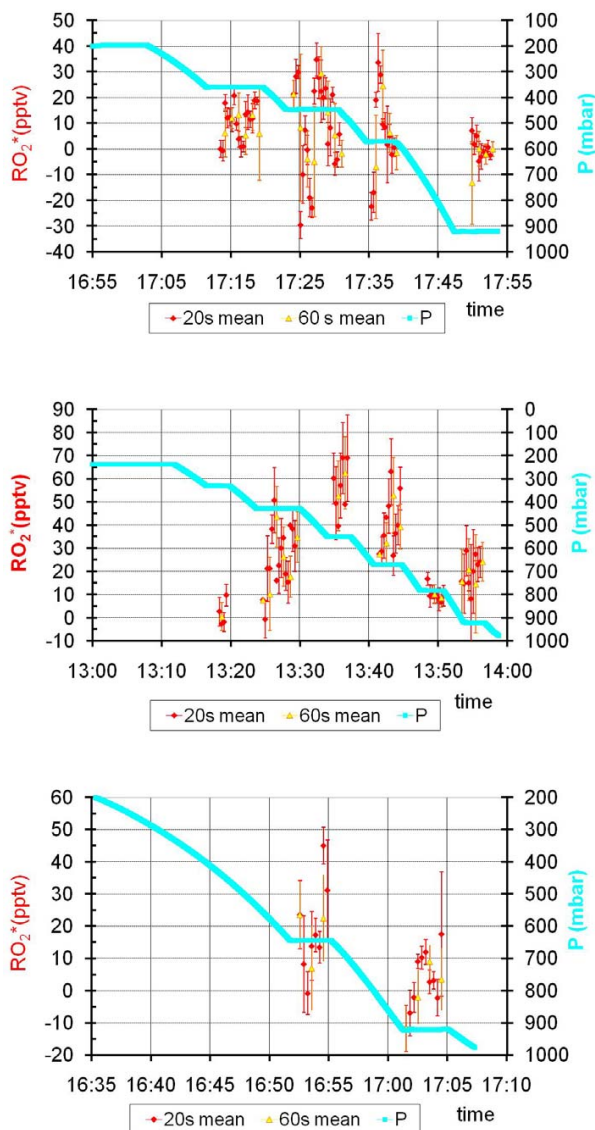


**Fig. 12.**  $\text{RO}_2^*$  mixing ratios measured in vertical profiles taken over Ouagadougou on the (a) 11 August 2006, (b) 13 August 2006, and (c) 15 August 2006.

are indicative of the influence of a biomass burning plume at the lower pressure levels (570–650 mbar). At the highest pressure layer, the trace gases  $\text{CO}$ ,  $\text{CO}_2$ ,  $\text{O}_3$ ,  $\text{NO}$  and  $\text{NO}_y$  reach 260, 379, 70, 0.160 and 2.8 ppbv, and 480, 390, 133, 0.25 and 8 ppbv on the 4 August and on the 13 August 2006, respectively. Interestingly,  $\text{RO}_2^*$  follow the general pattern, being higher and less variable on the 13 August (20–25 pptv) than on the 4 August 2006 (5–15 pptv), in spite of the higher  $\text{NO}$  concentrations and the lower radiation indicated by the lower values of  $j_{\text{NO}_2}$ , but in agreement with the larger  $\text{CO}$  and  $\text{HCHO}$  mixing ratios, the latter reaching 0.6 and 1.16 ppbv on the 4 and on the 13, respectively. The  $\text{NO}/\text{NO}_y$  ratio re-

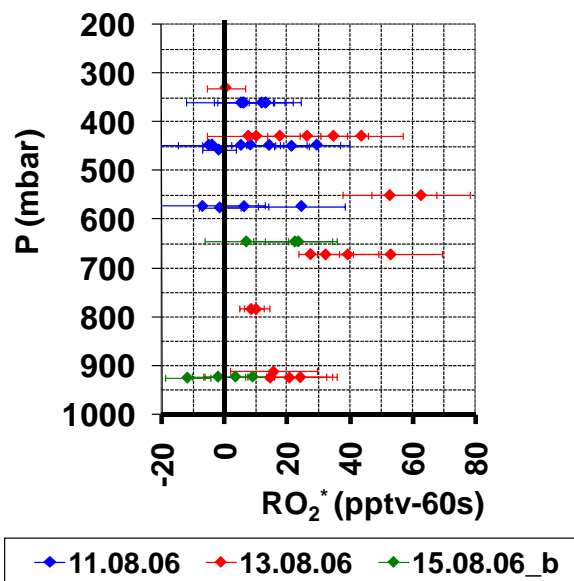


**Fig. 13.** Vertical profiles of  $\text{RO}_2^*$  mixing ratios measured over Ouagadougou. The 60 s mean values and the corresponding error bar are depicted. 15 August 2006b refers to the data measured on the flight in the afternoon.

mains quite low in both cases (around 0.04–0.05) indicating aged air masses. However,  $\text{HCHO}$  and acetone have both primary and secondary sources and can be therefore produced during the oxidation of the BB plume and act as source of peroxy radicals.

The  $\text{CO}$  satellite pictures in August from the TERRA-MOPITT (<http://eosweb.larc.nasa.gov>; Mari et al., 2008) as well as the  $\text{HCHO}$  from the ENVISAT-SCIAMACHY (Reeves et al., 2009; Wittrock et al., 2006) instruments indicate clearly the BB region in the proximity of the Gulf of Guinea and between  $5^\circ\text{N}$  and  $10^\circ\text{S}$  latitude. Mari et al. (2008) distinguish three different periods during the wet season in Africa, affecting the intrusions of southern hemispheric fire plumes in the Northern Hemisphere. These are characterised by advection patterns related to differences in the position and strength of the African Easterly Jet. According to this classification, the 13 August 2006 is within the second active phase, characterised by the advection of BB plumes out over the Atlantic in the mid troposphere, while the August corresponds to a break phase in which the pollutants emitted by the fires should be trapped over the continent and accumulate there until they reach convective regions located further north and are injected in the upper troposphere.

The vertical distribution of the trace gases measured on the 4 August is not as marked as on the 13 August which is less homogeneous and presents a clear layer between 500 and 650 mbar of higher concentrations and more photochemical activity. This agrees with the idea of an air mass which

has been in more recent contact with BB emissions and is transported at a lower pressure levels to the North as suggested by Mari et al. (2008) during the active phase. And conversely, on the 4 August, as indicated by the CO<sub>2</sub> concentrations, the air mass sampled seems to have been largely mixed vertically, while the effect of the BB emissions have been lost in importance as the air mass aged, in spite of its potential further enrichment with new fire emissions during the trapping over the continent. This also matches the lower photochemical activity observed. The trajectories calculated in the present work confirm this interpretation. Figure 11 shows the projection of the corresponding trajectory densities onto the ground and the longitude-height projection as defined in Sect. 2.3. For each projection the trajectory density is normalised to unity. On the 4 August 2006, the air sampled seems to originate from Nigeria in continental Africa, while at similar altitudes on the 13 August 2006 the air masses originate almost exclusively from the biomass burning area in Cameroon–Congo close to the Gulf of Guinea. According to these trajectories the air in the upper layers is transported from Central Africa.

### 3.3 Vertical distribution of RO<sub>2</sub><sup>\*</sup> over Ouagadougou

Figures 12 and 13 summarise the RO<sub>2</sub><sup>\*</sup> vertical profiles obtained on the 11, 13 and 15 August flights. RO<sub>2</sub><sup>\*</sup> up to 70 pptv with maximum mixing ratios between 400 and 700 mbar are observed. At a first glance the variability of the RO<sub>2</sub><sup>\*</sup> measurements seems to be large. Negative mixing ratios are occasionally calculated corresponding to signals measured close to the detection limit and presenting high variability around zero, as well as during very rapid changes in other trace species, clouds, humidity etc. In spite of the chemical meaningless of negative mixing ratios, these values are not removed as they are not caused by instrument failures and can provide useful information about radical variability and instrument response in a rapid changing environment. The analysis of data is however based on periods of stable conditions.

A closer analysis of the data confirms that the general radical variability is mostly explained by the presence of clouds, acting as a variable sink of radicals, and by the variability of other controlling trace species like NO<sub>x</sub>, CO and VOC (Fig. 14). The former is the case for the measurements taken on the 11 August at 445 and 570 mbar and on the 13 August close to the surface, where the low and variable values of  $j_{\text{NO}_2}$  ( $=0.006 \text{ s}^{-1}$ ) are indicative of the presence of clouds. In addition, variations up to 20 ppbv O<sub>3</sub>, 60 ppbv CO and 0.8 ppbv NO<sub>x</sub> are detected within the same pressure level in some of the flights. On the 15 August the NO<sub>y</sub> at 920 mbar vary up to 20 ppb. This indicates the existence of various vertical layers of different composition and photochemical activity.

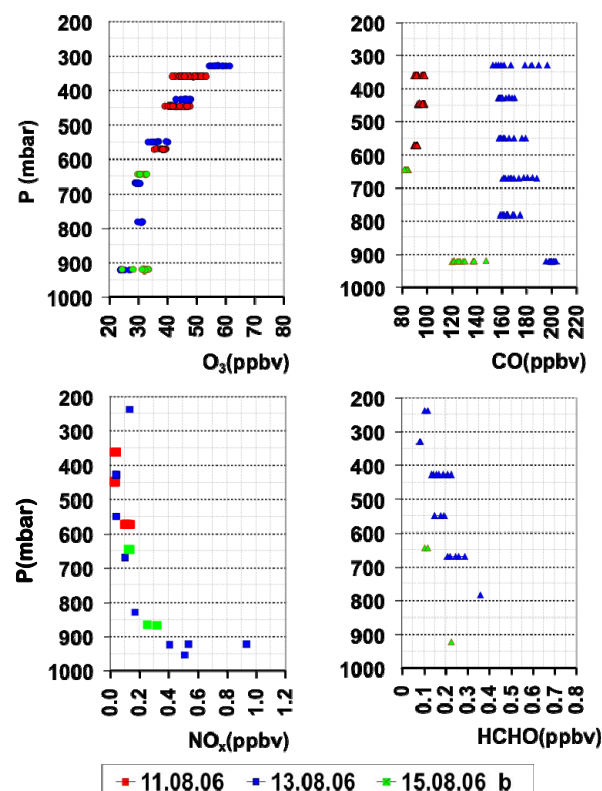


**Fig. 14.** Trace gas mixing ratios measured over Ouagadougou on the 11 August 2006, 13 August 2006 and 15 August 2006. The 15 August 2006b refers to the data of the afternoon flight.

### 3.4 Comparison with other measurements

Comparison with other aircraft measurements made during the campaign is possible on the 16 August 2006 flight, during which the DLR-Falcon and the BAe-146 flew close to each other at two different pressure levels. The flight is described more in detail by Reeves et al. (2009). A detailed quantitative comparison of the radical measurements is planned when the data of the PERCA onboard the BAe-146 become available. A preliminary comparison of the DUALER results with the HO<sub>2</sub> measured by LIF leads to a RO<sub>2</sub>/HO<sub>2</sub> 60:40 ratio.

A quantitative comparison with literature results requires a deep analysis of the individual data concerning the chemical composition of air masses, photochemical conditions, characteristics of the different platforms and measurement techniques. Generally, it is difficult to acquire this information at an adequate detail level, and even so, the normalisation of the different parameters and variables involved, prior to comparison is extremely complex. However, a simple qualitative comparison is of interest as it provides a first insight in the tropospheric vertical distribution and the range of values which can be expected under similar conditions. The data obtained within AMMA have been compared with the overview given in Cantrell et al. (2003a). These authors

reported a general vertical pattern for various measurement campaigns, sorted by latitude and season, with a mid lower troposphere concentration maximum around 3–4 km. As can be seen in Fig. 13, this description is in agreement with the values obtained between 800 and 450 mbar in Ouagadougou and presented in Sect. 3.3.

#### 4 Summary and conclusions

The total sum of peroxy radicals,  $\text{RO}_2^*$ , was successfully measured onboard of the DLR-Falcon instrumented aircraft during the West African monsoon period in summer 2006 by using a DUALER based on chemical amplification and a double reactor-detector system.

Air masses having different photochemical histories have been investigated.  $\text{RO}_2^*$  mixing ratios of high variability and up to 50–60 pptv were observed in the outflow of MCS. The variability is partly associated with the presence of clouds, which block and reflect photochemically active ultraviolet radiation. Occasionally, simultaneous unexpected increases of NO and  $\text{RO}_2^*$  are observed, indicating the presence of a radical precursor, which is related to NO emissions. Jaeglé et al. (1997b) interpreted the correlations between  $\text{NO}_y$  and CO observed at 8–12 km altitude over the central US as indication of the primary origin of  $\text{NO}_x$  being from convective transport of polluted boundary layer air. During the AMMA measurement campaign the  $\text{NO}_y$  and CO patterns often present similarities. However, the NO mixing ratios measured during the period by other aircrafts in the boundary layer are generally lower (Reeves et al., 2009), indicating that the  $\text{NO}_x$  observed must be to a large fraction related to lightning episodes rather than being exclusively convectively pumped to upper levels. Thunderstorms associated to MCS might also produce HOx and radical precursors as suggested by Zuo and Deng (1999). Lightning can cause decomposition of molecules like  $\text{O}_2$ ,  $\text{H}_2\text{O}$  and  $\text{N}_2$  and form reactive atoms and radicals which can recombine and lead to  $\text{H}_2\text{O}_2$ ,  $\text{O}_3$  and oxidized nitrogen species (Bhettanabhotla et al., 1985; Pinart et al., 1996; Coppens et al., 1998; Glindemann et al., 2004). It can be concluded that the MCS outflow air masses detected during the measurement campaign are still photochemically active. Simulations using a box model with simplified chemistry indicate local  $\text{O}_3$  production rates varying between 0.1 and 1.35 ppb  $\text{h}^{-1}$  within the MSC outflow and up to 0.3 ppb  $\text{h}^{-1}$  in potentially undisturbed upper tropospheric air masses. These results are consistent with other model simulations of MCS outflow within AMMA. The estimation of the global impact of MCS in the  $\text{O}_3$  production requires further investigation.

The photochemistry of air masses affected by biomass burning plumes has also been investigated by means of two vertical profiles taken at the coast close to Ghana. The differences in chemical composition agree reasonably with the expected advection patterns related to the different phases of the African Easterly Jet.  $\text{RO}_2^*$  mixing ratios around 20 pptv

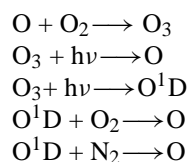
and with peak values up to 60 pptv within 400 and 500 mbar are detected, indicating the presence of photochemical active layers.

The final case study as part of this campaign was the investigation of vertical profiles measured over Ouagadougou. The data from the AMMA campaign yield a vertical distribution of  $\text{RO}_2^*$  having maximum mixing ratios between 450 and 700 mbar. This behaviour is similar to literature data taken under similar conditions and provides evidence for the enhanced free radical production in this pressure range. This presumably results from the uplifting of radical precursors from below.

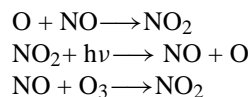
#### Appendix A

##### Chemistry of the box model

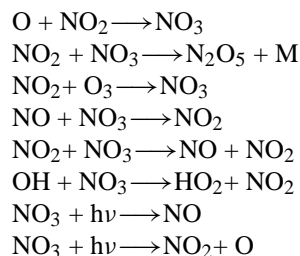
###### Ozone cycle



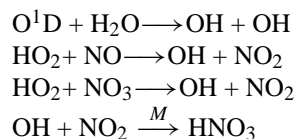
###### $\text{NO}_x$ cycle



###### $\text{NO}_3$ production and decay



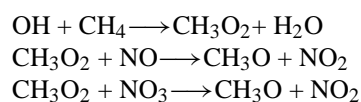
###### Hydroxyl radical

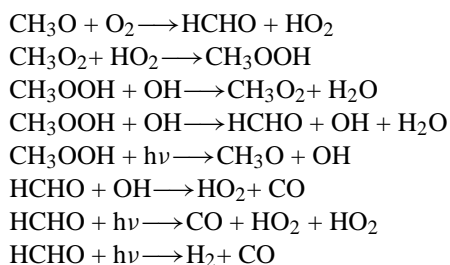


###### CO oxidation



###### Methane oxidation





All reaction rates are according to JPL-publication JPL 06-2 (Sander et al., 2006). The photolysis frequencies have been obtained using PhotoST (Burkert et al., 2003). PhotoST obtains the radiative fluxes from the radiative transfer model SCIATRAN (Rozanov et al., 2002), determines the actinic flux and performs the spectral integration of the product of the actinic flux, the absorption cross section and the quantum yield to derive the photolysis frequencies for all included photolytic reactions. The presence of cumulus clouds with a cloud top height well below the altitude of the aircraft has been assumed for this study. The reaction mechanism for isoprene decomposition (Meyer-Arnek et al., 2005) was additionally included in the box model. It bases on the simplification of the chemistry on the Master Chemical Mechanism version 3.1 (Saunders et al., 2003) focusing on the species being either involved in the  $\text{NO}_x$ - $\text{HO}_x$ -cycle or in the isoprene decay.

**Acknowledgements.** We would like to thank all the DLR colleagues and the Falcon crew for their support before, during and after the AMMA measurement campaign. Special thanks also to T. Hamburger for providing maps with trajectories. The DLR-Falcon operation was funded in part by DLR and the European Commission.

Based on a French initiative, AMMA was built by an international scientific group and is currently funded by a large number of agencies. It has been the beneficiary of a major financial contribution from the European Community Sixth Framework Research Programme. Detail information on scientific coordination and funding is available on the AMMA International web site at <http://www.amma-eu.org>.

Edited by: C. Reeves

## References

- Agustí-Panareda, A. and Beljaars, A.: ECMWF's contribution to AMMA, ECMWF Newsletter, No. 115, 19–27, Spring 2008.
- Ancellet, G., Leclair de Bellevue, J., Mari, C., Nedelec, P., Kukui, A., Borbon, A., and Perros, P.: Effects of regional-scale and convective transports on tropospheric ozone chemistry revealed by aircraft observations during the wet season of the AMMA campaign, *Atmos. Chem. Phys.*, 9, 383–411, 2009, <http://www.atmos-chem-phys.net/9/383/2009/>.
- Andrés Hernández, M. D., Burkert, J., Reichert, L., Stöbener, D., Meyer-Arnek J., Burrows, J. P., Dickerson, R. R., and Doddridge, B.: Marine boundary layer peroxy radical chemistry during the AEROSOLS99 campaign: measurements and analysis, *J. Geophys. Res.*, 106(D18), 20833–20846, 2001.
- Bechara, J., Borbon, A., Lambert, C., and Perros, P.: Evidence of deep convective transport of VOC trace gases in the upper tropical troposphere during the AMMA experiment, to be submitted, *ACP*, AMMA special issue, 2009.
- Bhetanabhotla, M. N., Crowell, B. A., Cowouvinos, A., et al.: Simulation of trace species production by lightning and corona discharge in moist air, *Atmos. Environ.*, 19, 1391–1397, 1985.
- Burkert, J., Behmann, T., Andrés Hernández, M.D., Weißenmayer, M., Perner, D., and Burrows, J.P.: Measurements of peroxy radicals in a forested area in Portugal, *Chemosphere Global Change Sci.*, 3(3), 327–338, 2001a.
- Burkert, J., Andrés-Hernández, M. D., Stöbener, D., Burrows, J. P., Weißenmayer, M., and Kraus, A.: Peroxy radical and related trace gas measurements in the boundary layer above the Atlantic Ocean, *J. Geophys. Res.*, 106(6), 5457 pp., 2001b.
- Burkert, J., Andrés-Hernández, M. D., Reichert, L., Meyer-Arnek, J., Doddridge, B., Dickerson, R. R., Muehle, J., Zahn, A., Carsey, T., and Burrows, J. P.: Trace gas and radical diurnal behavior in the marine boundary layer during INDOEX 1999, *J. Geophys. Res.*, 108 (D8), 8000, doi:10.1029/2002JD002790, 2003.
- Buxton, G. V., and Salmon G. A.: On the chemistry of inorganic free radicals in cloud water, *Prog. React. Kinet. Mec.*, 28, 257–297, 2003.
- Cantrell, C. A., Shetter, R. E., Gilpin, T. M., Calvert, J. G., Eisele, F. L., and Tanner, D. J.: Peroxy radical concentrations measured and calculated from trace gas measurements in the Mauna Loa Photochemistry Experiment 2, *J. Geophys. Res.*, 101, 14653–14664, 1996a.
- Cantrell, C. A., Shetter R. E., and Calvert, J. G.: Dual-Inlet chemical amplifier for atmospheric peroxy radical measurements, *Anal. Chem.*, 68, 4194–4199, 1996b.
- Cantrell, C. A., Edwards, G. D., Stephens, S., Mauldin, L., et al.: Peroxy radical behaviour during the Transport and Chemical Evolution over the Pacific (TRACE-P) campaign as measured aboard the NASA P-3B aircraft, *J. Geophys. Res.*, 108(D20), 8797, doi:10.1029/2003JD003674, 2003a.
- Cantrell, C. A., Edwards, G. D., Stephens, S., Mauldin, L., Kosciuch, E., Zondlo, M., and Eisele, F.: Peroxy radical observations using chemical ionization mass spectrometry during TOPSE, *J. Geophys. Res.*, 108(D6), 8371, doi: 10.1029/2002JD002715, 2003b.
- Cantrell, C. A., Mauldin, L., Zondlo, M., Eisele, F. et al.: Steady state free radical budgets and ozone photochemistry during TOPSE, *J. Geophys. Res.*, 108(D4), 8361, doi:10.1029/2002JD002198, 2003c.
- Carlsaw, N., Creasey, D. J., Heard, D. E., Lewis, A. C., McQuaid, J. B., Pilling, M. J., Monks, P. S., Bandy B. J., and Penkett S. A.: Modelling OH, HO<sub>2</sub>, and RO<sub>2</sub> in the marine boundary layer: 1. Model construction and comparison with field measurements, *J. Geophys. Res.*, 104(D23), 30241–30255, 1999.
- Cohan, D. S., Schultz, M. G., and Jacob, D. J.: Convective injection and photochemical decay of peroxides in the tropical upper troposphere: methyl iodide as a tracer of marine convection, *J. Geophys. Res.*, 104(D5), 5717–5724, 1999.
- Cooper, O. R., Stohl, A., Trainer, M., et al.: Large upper tropospheric ozone enhancements above midlatitude North America during summer: In situ evidence from the IONS and MOZAIC

- ozone measurement network, *J. Geophys. Res.*, 111, D24S05, doi:10.1029/2006JD007306, 2006.
- Coppens, F., Berton, R., Bondiou-Clergerie, A., and Gallimberti, I.: Theoretical estimate of NO<sub>x</sub> production in lightning corona, *J. Geophys. Res.*, 103, 10769–10785, 1998.
- Eneroth, K., Kjellstrom E., and Holmen, K.: A trajectory climatology for Svalbard; investigating how atmospheric flow patterns influence observed tracer concentrations, *Phys. Chem. Earth.*, 28, 1191–1203, 2003.
- Faloon, I., Tan, D., Brune, W. H., Jaeglé, L. D., Jacob, J., et al.: Observations of HO<sub>x</sub> and its relationship with NO<sub>x</sub> in the upper troposphere during SONEX, *J. of Geophys. Res.*, 105(D3), 3771–3783, 2000.
- Fleming, Z. L., Monks, P. S., Rickard, A. R., Heard, D. E., Bloss, W. J., Seakins, P. W., Still, T. J., Sommariva, R., Pilling, M. J., Morgan, R., Green, T. J., Brough, N., Mills, G. P., Penkett, S. A., Lewis, A. C., Lee, J. D., Saiz-Lopez, A., and Plane, J. M. C.: Peroxy radical chemistry and the control of ozone photochemistry at Mace Head, Ireland during the summer of 2002, *Atmos. Chem. Phys.*, 6, 2193–2214, 2006, <http://www.atmos-chem-phys.net/6/2193/2006/>.
- Fleming, Z. L., Monks, P. S., Rickard, A. R., Bandy, B. J., Brough, N., Green, T. J., Reeves, C. E., and Penkett, S. A.: Seasonal dependence of peroxy radical concentrations at a Northern hemisphere marine boundary layer site during summer and winter: evidence for radical activity in winter, *Atmos. Chem. Phys.*, 6, 5415–5433, 2006, <http://www.atmos-chem-phys.net/6/5415/2006/>.
- Folkens, I., Wennberg, P. O., Hanisco, T. F., Anderson, J. G., and Salawitch, R. J.: OH, HO<sub>2</sub>, and NO in two biomass burning plumes: Sources of HO<sub>x</sub> and implications for ozone production, *Geophys. Res. Lett.*, 24, 3185–3188, 1997.
- Gerbig, C., Kley, D., Volz-Thomas, A., et al.: Fast response resonance fluorescence CO measurements aboard the C-130: Instrument characterisation and measurements made during North Atlantic Regional Experiment 1993, *J. Geophys. Res.*, 101, 29229–29238, 1996.
- Gлиндemann, D. M., Edwards, M., and Schrems, O.: A Phosphine and methylphosphine production by simulated lightning – a study for the volatile phosphorus cycle and cloud formation in the earth atmosphere, *Atmos. Environ.*, 38, 6867–6874, 2004.
- Green, T. J., Brough, N., Reeves, C. E., Edwards, G. D., Monks P. S., and Penkett, S. A.: Airborne measurements of peroxy radicals using the PERCA technique, *J. Environ. Monitoring.*, 5, 75–83, 2003.
- Jaeglé, L., Jacob, D. J., Wennberg, P. O., et al.: Observed OH and HO<sub>2</sub> in the upper troposphere suggest a major source from convective injection of peroxides, *Geophys. Res. Lett.*, 24, 3181–3184, 1997a.
- Jaeglé, L., Jacob, D. J., Wang, Y., Weinheimer, A. J., Ridley, B. A., Campos, T. L., Sachse, G. W., and Hagen, D. E.: Sources and chemistry of NO<sub>x</sub> in the upper troposphere over the United States, *Geophys. Res. Lett.*, 25(10), 1705–1708, doi:10.1029/97GL03591, 1997b.
- Jaeglé, L., Jacob, D. J., Brune W. H., et al.: Ozone production in the upper troposphere and the influence of aircraft during SONEX: Approach of NO<sub>x</sub>-saturated conditions, *Geophys. Res. Lett.*, 26(20), 3081–3084, 1999.
- Jaeglé, L., Jacob, D. J., Brune W. H., and Wennberg, P. O.: Chemistry of HO<sub>x</sub> radicals in the upper troposphere, *Atmospheric Environment*, 35, 469–489, 2001.
- Kartal, D., Andrés-Hernández, M. D., Reichert, L., Schlager, H., and Burrows, J. P.: Characterisation of a DUALER instrument for the airborne measurement of peroxy radicals during AMMA 2006, to be submitted to ACP, 2009.
- Lelieveld, J. and Crutzen, P. J.: Role of deep cloud convection in the ozone budget of the troposphere, *Science*, 264(5166), 1759–1761, 1994.
- Lelieveld, J., Butler, T. M., Crowley, J. N., et al.: Atmospheric oxidation capacity sustained by a tropical forest, *Letters to Nature*, 452, 737–740, doi:10.1038/nature06870, 2008.
- Mari, C. H., Cailley, G., Corre, L., Saunois, M., Attié, J. L., Thouret, V., and Stohl, A.: Tracing biomass burning plumes from the Southern Hemisphere during the AMMA 2006 wet season experiment, *Atmos. Chem. Phys.*, 8, 3951–3961, 2008, <http://www.atmos-chem-phys.net/8/3951/2008/>.
- Mauersberger, G.: The influence of cloud chemistry on the budget of photo-oxidants, *Transactions on Ecology and the Environment*, 6, WIT Press, ISSN 1743-3541, 1995.
- McKeen, S. A., Gierczak, T., Burkholder J. B., et al.: The photochemistry of acetone in the upper troposphere: a source of odd-hydrogen radicals, *Geophys. Res. Lett.*, 24, 3177–3180, 1997.
- Meyer-Arnek, J., Ladstätter-Weißenmayer, A., Richter, A., Wittrock, F., and Burrows, J. P.: A study of the trace gas columns of O<sub>3</sub>, NO<sub>2</sub> and HCHO over Africa in September 1997, *Faraday Discuss.*, 130, 387–405, doi:10.1039/b502106p, 2005.
- Miyazaki, Y., Kita, K., Kondo, Y., et al.: Springtime photochemical ozone production observed in the upper troposphere over east Asia, *J. Geophys. Res.*, 107, 8398, doi:10.1029/2001JD000811, 2002.
- Monks P. S., Carpenter, L. J., and Penkett, S. A.: Night-time peroxy radical chemistry in the remote marine boundary layer over the Southern ocean, *Geophys. Res. Lett.*, 23(5), 535–538, 1996.
- Pinart, J., Smirdec, M., Pinart, M. E., et al.: Quantitative study of the formation of inorganic chemical species following corona discharge: I. Production of HNO<sub>2</sub> and HNO<sub>3</sub> in a composition controlled humid atmosphere, *Atmos. Environ.*, 30, 129–132, 1996.
- Prather, M. J., and Jacob, D. J.: A persistent imbalance in HO<sub>x</sub> and NO<sub>x</sub> photochemistry of the upper troposphere driven by deep tropical convection, *Geophys. Res. Lett.*, 24, 3189–3192, 1997.
- Reeves, C. E., Ancellet, G., Attie, J.-L., et al.: Chemical characterisation of the West Africa Monsoon during AMMA, ACP, to be submitted, 2009.
- Rozanov, V. V., Buchwitz, M., Eichmann, K.-U., de Beek R., and Burrows, J. P.: Sciatran – a new radiative transfer model for geophysical applications in the 240–2400 NM spectral region: the pseudo-spherical version, *Adv. Space. Res.*, 29(11), 1831–1835, 2002.
- Sander, S. P., Orkin, V. L., Kurylo, M. J., Golden, D. M., Huie, R. E., Kolb, C. E., Finlayson-Pitts, B. J., Molina, M. J., Friedl, R. R., Ravishankara, A. R., Moortgat, G. K., Keller-Rudek, H., Wine, P. H.: *Chemical Kinetics and Photochemical Data for Use in Atmospheric Studies Evaluation Number 15*, JPL publication 06–2, Jet Propulsion Laboratory, 2006.
- Saunders, S. M., Jenkin, M. E., Derwent, R. G., and Pilling, M. J.: Protocol for the development of the Master Chemical Mechanism, MCM v3 (Part A): tropospheric degradation of non-

- aromatic volatile organic compounds, *Atmos. Chem. Phys.*, 3, 161–180, 2003,  
<http://www.atmos-chem-phys.net/3/161/2003/>.
- Schlager, H., Konopka, P., Schulte, P., Schumann, U., Ziereis, H., Arnold, F., Klemm, M., Hagen, D., Whitefield, P., Ovarlez, J.: In situ observations of air traffic emission signatures in the North Atlantic flight corridor, *J. Geophys. Res.*, 102, 10739–10750, 1997.
- Schlager, H., Lichtenstern, M., Stock, P., et al.: Aircraft measurements of the chemical composition in fresh and aged outflow from Mesoscale Convective Systems in West Africa, ACP, to be submitted, AMMA Special Section, 2009.
- Schulte, P., Schlager, H., Schumann, U., Baughcum, St. L., Deidwig F.: NO<sub>x</sub> emission indices of subsonic long-range jet aircraft at cruise altitude: In situ measurements and predictions, *J. Geophys. Res.*, 102, 21431–21442, 1997.
- Seigneur, C. and Saxena, P.: The impact of cloud chemistry on photochemical oxidant formation, *Water Air Soil Poll.*, 24, 419–429, 1985.
- Shi, Q., Belair, S. D., Francisco, J. S., and Kais, S.: On the interactions between atmospheric radicals and cloud droplets: A molecular picture of the interface, *PNAS*, 100(17), 9686–9690, 2003.
- Stohl, A., Wotawa, G., Seibert, P., and Kromp-Kolb, H.: Interpolation errors in wind fields as a function of spatial and temporal resolution and their impact on different types of kinematic trajectories. *J. Appl. Meteor.*, 34, 2149–2165, 1995.
- Stohl, A. and Seibert, P.: Accuracy of trajectories as determined from the conservation of meteorological tracers. *Q. J. Roy. Met. Soc.*, 124, 1465–1484, 1998.
- Volz-Thomas A., Pätz, H.-W., Houben, N., Konrad, S., Mihelcic, D., Klüpfel, T., and Perner, D.: Inorganic trace gases and peroxy radicals during BERLIOZ at Pabstthum: An investigation of the photostationary state of NO<sub>x</sub> and O<sub>3</sub>, *J. Geophys. Res.*, 108(D4), 8248, doi:10.1029/2001JD001255, 2003.
- Wennberg, P. O., Hanisco, T. F., Jaeglé, L., Jacob, D. J., et al.: Hydrogen radicals, nitrogen radicals, and the production of O<sub>3</sub> in the upper troposphere, *Science*, 279, 49–53, 1998.
- Wittrock, F., Richter, A., Oetjen, H., Burrows, J. P., Kanakidou, M., Myriokefalitakis, S., Volkamer, R., Beirle, S., Platt U., and Wagner, T.: Simultaneous global observations of glyoxal and formaldehyde from space, *Geophys. Res. Lett.*, 33, L16804, doi:10.1029/2006GL026310, 2006.
- Zanis, P., Monks, P. S., Green, T. J., Schuepbach, E., Carpenter, L. J., Mills, G. P., Rickard, A. R. and Penkett, S. A.: Seasonal variation of peroxy radicals in the lower free troposphere based on observations from the FREE Tropospheric Experiments in the Swiss Alps, *Geophys. Res. Lett.*, 30(10), 1497, doi:10.1029/2003GL017122, 2003.
- Zuo, Y. and Deng, Y.: Evidence for the production of hydrogen peroxide in rainwater by lightning during thunderstorms, *Geochim. Cosmochim. Ac.*, 63(19/20), 3451–3455, 1999.
- Ziereis, H., Schlager, H., Schulte, P., van Velthoven, P., and Slemr, F.: Distributions of NO, NO<sub>x</sub>, and NO<sub>y</sub> in the upper troposphere and lower stratosphere between 28 and 61° N during POLI-NAT 2, *J. Geophys. Res.*, 105, 3653–3664, 2000.